

Green Chemistry

DOI: 10.1002/ange.200500346

**Open-Framework Chalcogenides as Visible-Light Photocatalysts for Hydrogen Generation from Water\*\***

*Nanfeng Zheng, Xianhui Bu, Hiep Vu, and Pingyun Feng\**

The concern over the limited supply and the environmental effects of fossil fuels has led to increasing efforts directed towards the development of semiconductor photocatalysts for the production of hydrogen from water by using solar energy.<sup>[1–6]</sup> However, despite years of effort in this area of research, there are still many challenges that need to be met before such a photocatalytic process becomes economically feasible. The current limitations include the inadequate conduction-band energy levels for the photoreduction of

[\*] N. Zheng, H. Vu, Prof. P. Feng

Department of Chemistry  
University of California  
Riverside, CA 92521 (USA)  
Fax: (+1) 951-827-4713  
E-mail: pingyun.feng@ucr.edu

Prof. X. Bu  
Department of Chemistry and Biochemistry  
California State University  
1250 Bellflower Blvd.  
Long Beach, CA 90840 (USA)

[\*\*] We thank the NSF-DMR (P.F.) and the donors of the Petroleum Research Fund (administered by the ACS; X.B. and P.F.) for support of this work. P.Y. is an Alfred P. Sloan research fellow, Beckman Young Investigator, and Camille Dreyfus Teacher-Scholar.

water and wide band gaps that correspond to UV light rather than visible light.<sup>[7]</sup>

Doping transition-metal cations or nitrogen anions into oxides is a commonly used strategy to create energy levels between valence and conduction bands so that the photocatalysts can be active in the visible-light region.<sup>[8–11]</sup> However, if the conduction-band level of a semiconductor is lower than the water-reduction potential, the doped semiconductor is usually photocatalytically inactive with respect to water reduction.

To overcome the above limitations and create a new generation of photocatalysts, it is necessary to develop a synthetic strategy that is capable of the systematic modification of both the electronic band gap and the energy level of each individual band. In addition, it is highly desirable to have a photocatalyst with a large number of active sites so as to increase quantum efficiency. Towards these goals, we have been developing methods for the synthesis of crystalline porous chalcogenide semiconductors with the expectation that such materials will have promising photocatalytic properties, particularly in the visible-light region.

We envision several unique advantages of photocatalysts based on crystalline porous semiconductors. By controlling framework architecture, it is possible to tune the band structure (both band positions and gap) of an open-framework solid within a given compositional domain. The open-framework construction also helps to increase the number of active reaction sites owing to a high surface area. The rate of charge recombination of the electron-hole pair is likely to be reduced because unlike a dense solid, the electron or hole does not need to travel all the way to the external surface of the catalyst particle for a reaction to occur. In addition to functioning as efficient photocatalysts on the basis of their framework composition and architecture, porous crystalline semiconductors can also serve as hosts for the incorporation of metal complexes, dyes, or other optically active species into their cavities. The synergetic effects in such hybrid materials are often highly desirable for enhancing photocatalytic efficiency.

Unfortunately, whereas open-framework materials have been extensively studied during the past several decades,<sup>[12–14]</sup> the vast majority of them are insulating oxides and therefore unsuitable for photocatalytic applications. There are also very few examples of hybrid materials between crystalline porous semiconductors and light-absorbing metal complexes (or dyes). Recently, a large family of crystalline chalcogenide open frameworks were developed.<sup>[15–19]</sup> These materials integrate tunable band gaps with an open-framework architecture and are potential candidates for efficient photocatalysts, particularly in the visible-light region. Herein we report photocatalytic properties of some select crystalline open-framework sulfides and demonstrate their unique features, particularly in comparison with some related dense semiconductors. This work represents our first step towards the development of efficient photocatalysts based on crystalline porous semiconductors.

The porous chalcogenides in this study were synthesized from solutions comprising  $\text{In}^{3+}$  and  $\text{S}^{2-}$  ions and one type of transition-metal cation (e.g.,  $\text{Cd}^{2+}$ ,  $\text{Zn}^{2+}$ ,  $\text{Mn}^{2+}$ ,  $\text{Cu}^+$ ) under

hydrothermal conditions. Two series of materials (denoted ICF-*m* and UCR-*m*) have been made. The ICF-*m* series contains hydrated inorganic cations (e.g.,  $\text{Li}^+$ ,  $\text{Na}^+$ ) as extra-framework charge-balancing species and the UCR-*m* series contains protonated organic amines. The host framework of these materials is built from corner-sharing nanosized super-tetrahedral clusters denoted as  $\text{Tn}$ , in which *n* is the number of metal-sulfide layers in each cluster (Figure 1). UCR-7 has two interpenetrating cubic ZnS type lattices with T3 clusters

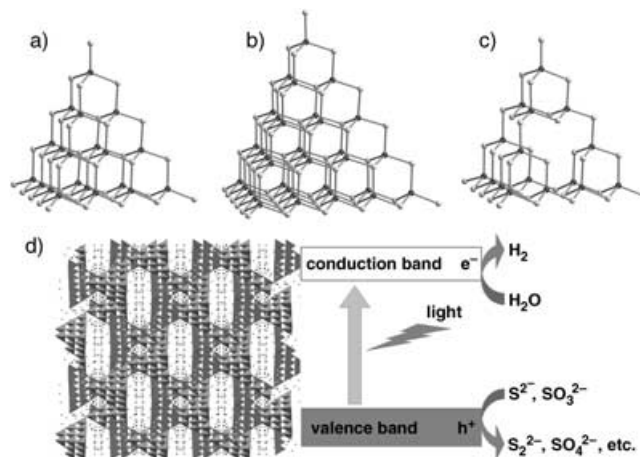


**Figure 1.** The structural and schematic diagrams of representative supertetrahedral clusters, chalcogenide frameworks, and their photocatalytic activity: a) T4 cluster; b) T5 cluster; c) coreless T4 cluster; d) the 3D diamond-type superlattice in ICF-5CuInS-Na: unconnected spheres are water molecules and  $\text{Na}^+$  sites.

( $\text{In}_{10}\text{S}_{18}^{6-}$ ) at the tetrahedral nodes and UCR-20 has the sodalite-type structure with T2 clusters ( $\text{M}_4\text{S}_8^{4-}$ ,  $\text{M} = \text{In/Ge}$ ,  $\text{In/Sn}$ ,  $\text{Ga/Ge}$ , and  $\text{Ga/Sn}$ ) at the tetrahedral nodes. ICF-5, ICF-17, and ICF-22 all contain two interpenetrating cubic ZnS type lattices; however, tetrahedral nodes are occupied by T4 clusters (e.g.,  $\text{Cu}_3\text{In}_{17}\text{S}_{33}^{10-}$ ,  $\text{Cd}_4\text{In}_{16}\text{S}_{33}^{10-}$ ) in ICF-5, T5 clusters (e.g.,  $\text{Zn}_{13}\text{In}_{22}\text{S}_{54}^{16-}$ ) in ICF-17, and the coreless T4 cluster ( $\text{In}_{16}\text{S}_{32}^{16-}$ ) in ICF-22 (Figure 1). The size as measured between corner sulfur sites is 1.6 nm and 2.0 nm for T4 and T5 clusters, respectively. All these materials contain channels and cavities within 3D frameworks. A detailed discussion on the syntheses and structures of these materials was given elsewhere.<sup>[18–19]</sup>

A variety of compositions can be realized for these materials through the incorporation of different transition-metal cations, which provides a convenient route for the modification of the band gap. Figure 2 shows the UV/Vis-near-IR diffuse reflectance spectra of different ICF-*m* and UCR-*m* compounds and demonstrates how the band gap can be tuned from 2.0 to 3.6 eV. ICF-5InCuS-Na (formula:  $\text{Na}_{14}\text{In}_{17}\text{Cu}_3\text{S}_{35} \cdot x\text{H}_2\text{O}$ ) is particularly interesting as it is compositionally related to  $\text{CuInS}_2$ , which is one of the most efficient photovoltaic materials. The introduction of  $\text{Cu}^+$  cations into the InS framework dramatically decreases the band gap to 2.0 eV, which makes this material particularly suitable for applications in the visible-light region.

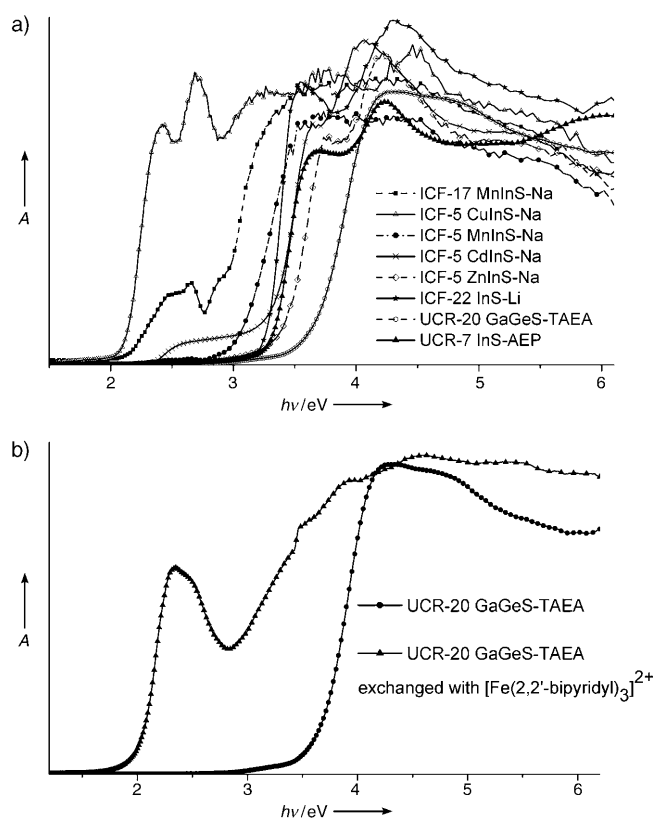


**Figure 2.** a) UV/Vis diffuse reflectance spectra of different open-framework chalcogenide materials. b) UV/Vis diffuse reflectance spectra of UCR-20GaGeS-TAEA before and after overnight ion exchange with 0.1 M  $[\text{Fe}(2,2'\text{-bipyridine})_3]^{2+}$  solution. Data were measured on a Shimadzu UV-3101PC double-beam, double-monochromator spectrophotometer.  $\text{BaSO}_4$  powder was used as reference (100% reflectance) and sometimes as base material for the coating of samples. Absorption ( $\alpha/S$ ) data were calculated from the reflectance data by using the Kubelka–Munk function:  $\alpha/S = (1-R)^2/R$ , in which  $R$  is the reflectance at a given wavelength,  $\alpha$  is the absorption coefficient, and  $S$  is the scattering coefficient.

A comparative study of porous sulfides and compositionally related dense phases showed that porous sulfides have a much higher photocatalytic activity. As shown in Figure 3a, about  $18 \mu\text{mol h}^{-1} \text{g}^{-1}$  of  $\text{H}_2$  gas was produced over the ICF-5CuInS-Na catalyst under irradiation with the visible light. This activity was maintained for over 96 h and more than  $890 \mu\text{mol}$  of  $\text{H}_2$  gas evolved during this period. The turnover number—defined as the ratio between the moles of reacted electrons and the amount of the photocatalyst—exceeded 15 after 96 h, which indicates that the reaction proceeds photocatalytically. There was no difference in XRD patterns of the catalyst before and after the reaction. However, the light reddish reaction mixture might be related to the slow degradation of the catalyst. The quantum efficiency for ICF-5CuInS-Na was determined to be about 3.7% at 420 nm. Even though the number is lower than the quantum yield ( $\approx 35\%$ ) of the well-known Pt/CdS photocatalyst, the efficiency is a considerable improvement on two anhydrous dense phases with similar compositions:  $\text{CuInS}_2$  with the cubic ZnS structure;  $\text{CuIn}_5\text{S}_8$  with the spinel structure. The quan-

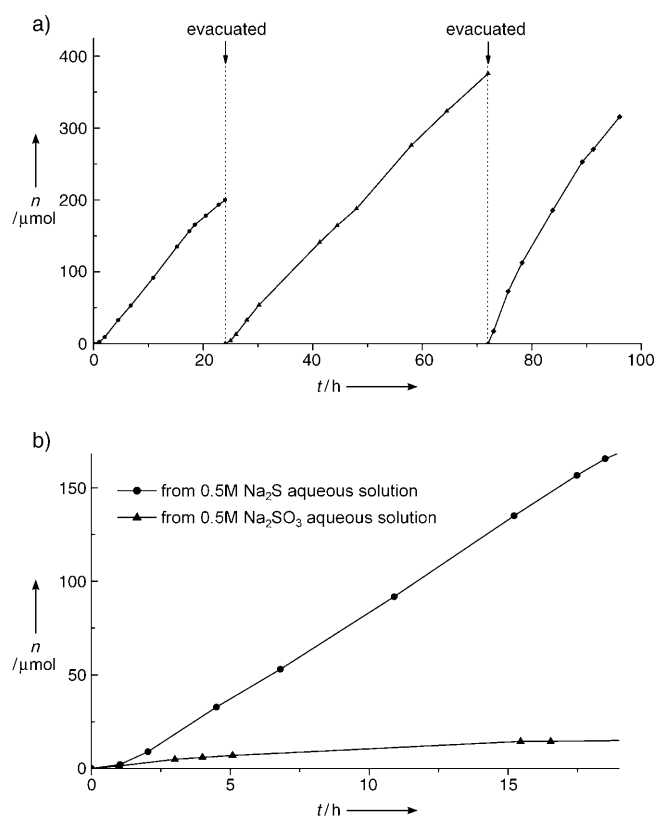


**Figure 3.** a) Photocatalytic  $\text{H}_2$  evolution from an aqueous solution of  $\text{Na}_2\text{S}$  (0.5 M) over ICF-5 CuInS-Na (0.5 g);  $t$ : irradiation time,  $n$ : amount of  $\text{H}_2$ . b) Comparison of photocatalytic evolution of  $\text{H}_2$  from an aqueous solution of  $\text{Na}_2\text{S}$  (0.5 M) and an aqueous solution of  $\text{Na}_2\text{SO}_3$  (0.5 M) over ICF-5CuInS-Na (0.5 g). Light source: 300-W Xe lamp,  $\lambda > 420 \text{ nm}$ .

tum yield of  $\text{CuIn}_5\text{S}_8$  with cocatalyst  $\text{Ag}_2\text{S}$  was reported smaller than 0.02% at 460 nm and  $25^\circ\text{C}$  while the efficiency of  $\text{CuInS}_2$  was even lower.<sup>[20]</sup>

When the photocatalytic reaction with ICF-5CuInS-Na was repeated under similar conditions but with 0.5 M  $\text{Na}_2\text{SO}_3$  as the sacrificial agent instead of 0.5 M  $\text{Na}_2\text{S}$ , the amount of hydrogen produced was reduced substantially to about one tenth of that from the  $\text{Na}_2\text{S}$  solution (Figure 3b). The production of hydrogen was negligible after 15 h of irradiation, which suggests that the  $\text{SO}_3^{2-}$  ion is a less effective sacrificial agent than the  $\text{S}^{2-}$  ion.

It is worth noting that ICF-5CuInS-Na is photocatalytically active without the use of a cocatalyst such as Pt. We have also observed hydrogen evolution over other porous chalcogenides such as ICF-17MnInS-Na (formula:  $\text{Na}_{16}\text{Mn}_{13}\text{In}_{22}\text{S}_{54} \cdot x\text{H}_2\text{O}$ ) or ICF-5CdInS-Na (formula:  $\text{Na}_{10}\text{Cd}_4\text{In}_{16}\text{S}_{33} \cdot x\text{H}_2\text{O}$ ) upon irradiation with visible light, again without any cocatalyst. Unlike typical dense semiconductors,<sup>[21–23]</sup> the presence of the Pt cocatalyst does not show an observable effect on the photocatalytic activity of these porous chalcogenides.

It is possible to engineer the band gap in the construction of an open framework. Similar to the effect that a decrease in conjugation leads to an increased energy gap in an organic

conjugated system, the generation of porosity in crystalline semiconductors leads to an increase in the band gap and energy level of the conduction band. For example,  $\text{NaInS}_2$  is a layered dense phase with a band gap of 2.3 eV;<sup>[24]</sup> in comparison, the band gap of ICF-22InS-Li (formula:  $\text{LiInS}_2 \cdot x\text{H}_2\text{O}$ ) is 3.3 eV (Figure 2 a).

An increase in the energy of the conduction-band level, which may be made possible through the construction of a porous architecture, can help generate water-reduction photocatalysts from inactive semiconductors in a compositional domain with an inadequate conduction energy level. For example, even under UV irradiation, no photocatalytic activity for the evolution of hydrogen was observed from  $\text{In}_2\text{S}_3$ , a 3D dense structure.<sup>[24]</sup> However, UCR-7InS-AEP (framework formula:  $\text{In}_{10}\text{S}_{18}^{6-}$ ; AEP = protonated 1-(2-aminoethyl)piperazine) showed high photocatalytic activity for the hydrogen evolution under UV irradiation (Figure 4). In

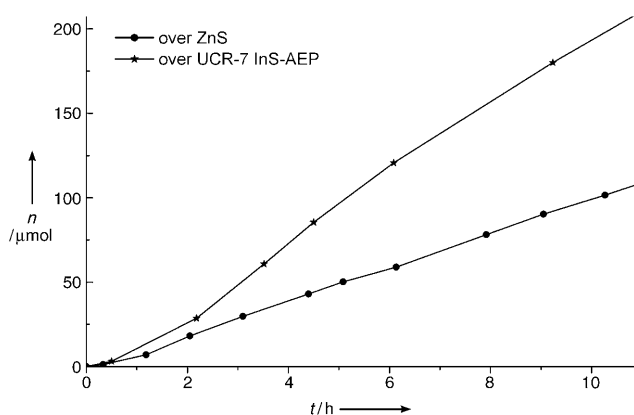


**Figure 4.** Comparison of photocatalytic  $\text{H}_2$  evolution from 0.5 M  $\text{Na}_2\text{SO}_3$  aqueous solution over 0.5 g UCR-7InS-AEP and ZnS. Light source, 300-W Xe lamp;  $t$ : irradiation time,  $n$ : amount of  $\text{H}_2$ .

the absence of any cocatalyst and under similar conditions, its activity is better than that of ZnS, a well-known UV-active photocatalyst.<sup>[25]</sup> A similar structural effect on photocatalytic activity has also been observed among oxide materials. For example, dense  $\text{Nb}_2\text{O}_5$  shows little activity for the photo-reduction of water due to its low conduction band. In comparison, a number of layered and tunneled structures based on niobium oxide are highly active in the UV region.<sup>[4]</sup>

In addition to the engineering of the band gap, the construction of an open framework makes it possible to create new composite visible-light photocatalysts by integrating porous semiconducting frameworks with optically active organic molecules or metal complexes. Upon incorporation into the pores of open-framework materials, dye molecules can function as sensitizers to enhance visible-light absorption and the subsequent transfer of energy to the semiconducting framework. The open-framework architecture can accommodate a high concentration of dye sensitizers, which is difficult to achieve by coating the surface of dense materials. The hybridization of crystalline porous semiconductors and metal complexes (or dyes) has the potential to make highly efficient

use of solar energy and therefore significantly improve the photocatalytic efficiency.

In this work, the  $[\text{Fe}(\text{2,2'}\text{-bipyridine})_3]^{2+}$  complex was incorporated into UCR-20GaGeS through ion exchange. XRD patterns before and after ion exchange were nearly identical; however, the absorption of the hybrid material was extended from the UV region to the visible-light region (Figure 2 b). The resulting red sample showed photocatalytic activity for the generation of hydrogen under irradiation with visible light ( $\lambda > 420 \text{ nm}$ ) for at least 24 h with  $\text{SO}_3^{2-}$  ions as the sacrificial agent. In comparison, the photocatalytic activity of both  $[\text{Fe}(\text{2,2'}\text{-bipyridine})_3]^{2+}$  and UCR-20GaGeS-TAEA was also studied with  $\text{SO}_3^{2-}$  ions as the sacrificial agent (TAEA = protonated tris(2-aminomethyl)amine). They did not show observable activity in the visible-light region even though UCR-20 GaGeS-TAEA was found to exhibit activity under the UV light. Only after ion exchange of  $[\text{Fe}(\text{2,2'}\text{-bipyridine})_3]^{2+}$  into UCR-20 did the resulting hybrid material show activity in visible light region.

In conclusion, a series of open-framework chalcogenides have been demonstrated to be efficient photocatalysts for the reduction of water. We have shown that novel hybrids of crystalline porous semiconductors and light-absorbing metal complexes can be prepared and these materials exhibit unique optical and photocatalytic properties. Compared with dense semiconductors, these porous semiconductors have received much less attention and their photocatalytic efficiency still requires further optimization. However, the unique advantages of porous semiconductors, such as having a high surface area and the easy incorporation of light sensitizers, provide new opportunities that can be explored to maximize photocatalytic efficiency, particularly in the visible-light region. We anticipate that the unique effects and advantages associated with the porous architecture are relevant to both porous sulfide and oxide semiconductor materials, which promise a new generation of photocatalysts for applications such as water reduction or splitting.

## Experimental Section

The photocatalytic reactions were performed in a pyrex reaction cell connected to a closed gas-evacuation and circulation system.

In a typical procedure, the catalyst (0.5 g) was suspended in a solution of  $\text{Na}_2\text{S}$  or  $\text{Na}_2\text{SO}_3$  (0.5 M, 270 mL). After the system had been evacuated, Ar gas was introduced into the reaction cell until a pressure of about 9.3 kPa was reached. The catalyst suspension was then irradiated with a 300 W Xe lamp equipped with an optical cut-off filter ( $\lambda > 420 \text{ nm}$ ) and a heat-absorbing filter. The amount of  $\text{H}_2$  produced was analyzed by using an online gas chromatograph equipped with a thermal-conductivity detector (TCD). Quantum yield was measured at 420 nm by using a band-pass filter with a half width of 9.8 nm. The number of incident photons was determined by a chemical actinometry based on potassium ferrioxalate.

Received: January 29, 2005

Published online: July 22, 2005

**Keywords:** green chemistry · heterogeneous catalysis · microporous materials · photochemistry · reduction

- [1] A. Fujishima, K. Honda, *Nature* **1972**, 238, 37–38.
- [2] Z. G. Zou, J. H. Ye, K. Sayama, H. Arakawa, *Nature* **2001**, 414, 625–627.
- [3] T. Takata, A. Tanaka, M. Hara, J. N. Kondo, K. Domen, *Catal. Today* **1998**, 44, 17–26.
- [4] K. Domen, J. N. Kondo, M. Hara, T. Takata, *Bull. Chem. Soc. Jpn.* **2000**, 73, 1307–1331.
- [5] A. Kudo, *Catal. Surv. Asia* **2003**, 7, 31–38.
- [6] M. Ashokkumar, *Int. J. Hydrogen Energy* **1998**, 23, 427–438.
- [7] J. R. Bolton, *Science* **1978**, 202, 705–711.
- [8] A. K. Ghosh, H. P. Maruska, *J. Electrochem. Soc.* **1977**, 124, 1516–1522.
- [9] W. Choi, A. Termin, M. R. Hoffmann, *J. Phys. Chem.* **1994**, 98, 13669–13679.
- [10] R. Asahi, T. Morikawa, T. Ohwaki, K. Aoki, Y. Taga, *Science* **2001**, 293, 269–271.
- [11] S. U. M. Khan, M. Al-Shahry, W. B. Ingler, *Science* **2002**, 297, 2243–2245.
- [12] D. W. Breck, *Zeolite Molecular Sieves*, Wiley, New York, **1984**.
- [13] M. E. Davis, *Nature* **2002**, 417, 813–821.
- [14] A. K. Cheetham, G. Ferey, T. Loiseau, *Angew. Chem.* **1999**, 111, 3466–3492; *Angew. Chem. Int. Ed.* **1999**, 38, 3268–3292.
- [15] R. L. Bedard, S. T. Wilson, L. D. Vail, J. M. Bennett, E. M. Flanigen in *Zeolites: Facts, Figures, Future. Proceedings of the 8th International Zeolite Conference* (Eds.: P. A. Jacobs, R. A. van Santen) Elsevier, Amsterdam, **1989**, p. 375–387.
- [16] a) H. Li, A. Laine, M. O’Keefe, O. M. Yaghi, *Science* **1999**, 283, 1145–1147; b) H. Li, J. Kim, T. L. Groy, M. O’Keefe, O. M. Yaghi, *J. Am. Chem. Soc.* **2001**, 123, 4867–6868.
- [17] a) C. L. Cahill, Y. Ko and J. B. Parise, *Chem. Mater.* **1998**, 10, 19–21; b) C. L. Cahill, J. B. Parise, *J. Chem. Soc. Dalton Trans.* **2000**, 1475–1482.
- [18] a) N. Zheng, X. Bu, B. Wang, P. Feng, *Science* **2002**, 298, 2366–2399; b) C. Wang, Y. Li, X. Bu, N. Zheng, O. Zivkovic, C. Yang, P. Feng, *J. Am. Chem. Soc.* **2001**, 123, 11506–11507.
- [19] N. Zheng, X. Bu, P. Feng, *Nature* **2003**, 426, 428–432.
- [20] M. Matsumura, S. Furukawa, Y. Saho, T. Hiroshi, *J. Phys. Chem.* **1985**, 89, 1327–1329.
- [21] J.-F. Reber, M. Rusek *J. Phys. Chem.* **1986**, 90, 824–834.
- [22] K. Kobayakawa, A. Teranishi, T. Tsurumaki, Y. Sato, A. Fujishima, *Electrochim. Acta* **1992**, 37, 465–467.
- [23] A. Kudo, I. Tsuji, H. Kato, *Chem. Commun.* **2002**, 1958–1959.
- [24] A. Kudo, A. Nagane, I. Tsuji, H. Kato, *Chem. Lett.* **2002**, 882–883.
- [25] J.-F. Reber, K. Meier, *J. Phys. Chem.* **1984**, 88, 5903–5913.